international wound journal

International Wound Journal ISSN 1742-4801

ORIGINAL ARTICLE

Transplantation of BMSCs expressing hVEGF$_{165}$/hBD3 promotes wound healing in rats with combined radiation-wound injury

Zhangquan Xia[1,2], Congji Zhang[1], Yi Zeng[1], Tao Wang[3], Guoping Ai[3]

1 Department of Stomatology, Southwest Hospital, Third Military Medical University, Chongqing, China
2 Department of Stomatology, No 291 Hospital of the People's Liberation Army, Baotou, China
3 Department of Radiation Medicine, Institute of Combined Injury, State Key Laboratory of Trauma, Burns and Combined Injury, Third Military Medical University, Chongqing, China

Key words
Bone-marrow-derived mesenchymal stem cells; Human beta-defensin; Human vascular endothelial growth factor 165; Wound healing

Correspondence to
Dr C Zhang, MD, Department of Stomatology, Southwest Hospital, Third Military Medical University, 30 Gaotanyan Street, Chongqing 400038, China
E-mail: zhangcongji@tmmu.edu.cn

doi: 10.1111/j.1742-481X.2012.01090.x

Xia Z, Zhang C, Zeng Y, Wang T, Ai G. Transplantation of BMSCs expressing hVEGF$_{165}$/hBD3 promotes wound healing in rats with combined radiation-wound injury. Int Wound J 2014; 11:293–303

Abstract

The combined radiation-wound injury is a refractory wound with decreased number or dysfunction of repairing cells and growth factors. This remains a challenge in clinical practice. The object of this study is to evaluate the therapeutic efficacy of a combination of human vascular endothelial growth factor 165 (hVEGF$_{165}$) and human beta-defensin 3 (hBD3) in the treatment of such wounds. A plasmid-carrying hVEGF$_{165}$ gene and hBD3 gene was used to transfect rat bone-marrow-derived mesenchymal stem cells (BMSCs). The supernatant from the modified BMSCs significantly promoted the proliferation and cell migration of human endothelial cells and it also inhibited the growth of bacteria and fungus, demonstrating the successful expression of the transfected genes. The hVEGF$_{165}$/hBD3-modified BMSCs were then injected into the sites of combined radiation-wound injury on rats. It demonstrated that wound-healing time was shortened significantly in the treated rats. The granulation tissue formation/maturation, skin appendage regeneration and collagen deposition were also improved significantly. Strong expression of hVEGF$_{165}$ and hBD3 was detected in the wound surface at early stage of the healing. The results indicate that topical transplantation of hVEGF$_{165}$/hBD3-modified BMSCs promoted wound healing, and this gene therapy strategy presents a promising approach in the treatment of refractory wounds such as the combined radiation-wound injury.

Introduction

With the increasing use of nuclear power in our life, the concerns about the ionising radiation damage to the human body are also growing. Ionising radiation damage could result from nuclear power plant accidents, radiation therapy for malignancy, prolonged fluoroscopy, inhalation of excess radionuclides and nuclear explosions. The damage is harder to heal than normal wounds and remains a challenge in clinical practice (1–3). There is a coordinated healing process following a normal wound; this involves an interacting network of multiple cells, cytokines and extracellular matrix. During normal wound healing, many cytokines and growth factors are produced through para- or autocrine. These factors mediate and regulate a cascade reaction to promote wound healing.

Key Messages

- the combined radiation-wound injury is harder to heal than normal wounds due to decreased number or dysfunction of repairing cells and reduction in growth factors, collagen synthesis, and inflammatory cells
- a gene therapy strategy with locally injection of human vascular endothelial growth factor 165 (hVEGF165) and human beta-defensin 3 (hBD3) modified bone marrow-derived mesenchymal stem cells (BMSCs) presents a promising approach in the treatment

In combined radiation-wound injury, the wound surface is refractory to healing, due to decreased number or dysfunction

of repairing cells and reduction in growth factors, collagen synthesis and inflammatory cells (4).

During wound healing, bone-marrow-derived mesenchymal stem cells (BMSCs) migrate to the wound or inflammatory site, contributing to tissue regeneration and reconstruction. They stimulate progenitor cells to proliferate and differentiate, secrete growth factors and remodel tissues. Furthermore, BMSCs exert special immunoregulatory and anti-inflammatory actions on wound closure (5–8). Vascular endothelial growth factor (VEGF) acts as a mitogen of endothelial cells, a chemotactic mediator and a vascular permeability inducer. It plays multiple roles in the wound-healing cascade, angiogenesis, endothelial formation and collagen deposition. $VEGF_{165}$ is the most active isoform of VEGF. As angiogenesis is critical to wound healing, the use of VEGF alone or in combination with other factors has become the focus in wound therapy of wound (9–13). Persistent topical infection is one of the causes for refractory wound surface. It has been demonstrated that infection is closely associated with wound-healing impairment when the number of microorganisms is greater than 10^6/g tissue (14). Human beta-defensin 3 (hBD3) plays an important role in preventing and treating human infectious diseases. It exhibits antibacterial activity for gram-positive bacteria even at very low doses. Meanwhile, hBD3 does not cause haemolysis or tissue damage, and its antibacterial activity is insensitive to ionic concentration (15,16). Studies also provided evidence that hBD3 immunomodulates T-lymphocytes and immature dendritic cells. It plays an important role in both congenital and acquired immunity (17,18). In addition, recombinant hBD3 was demonstrated to have the same antibacterial and biological properties as the natural hBD3 (19).

We hypothesise that there may be combined therapeutic efficacy of hVEGF and hBD3 in the treatment of combined radiation-wound injury. So we constructed a recombinant eukaryotic expression plasmid, which expresses $hVEGF_{165}$ and hBD3 simultaneously. The plasmid was transfected into rat BMSCs, which were then injected subcutaneously into the site of combined radiation-wound injury on rats. The results demonstrated that this *ex vivo* gene therapy strategy significantly promoted wound healing.

Materials and methods

RNA isolation and reverse transcription

Total RNA was isolated from cells and tissues using the standard acid phenol/guanidine isothiocyanate procedure (Roche, Indianapolis, IN) and was reverse transcribed using the M-MLV reverse transcription kit (Invitrogen, Carlsbad, CA).

Construction of recombinant eukaryotic expression vectors

$hVEGF_{165}$ cDNA was amplified from HL-60 cells. *Bsp*HI and *Hin*dIII endonuclease sites were introduced to the 5′ end and 3′ end of the $hVEGF_{165}$ cDNA through the polymerase chain reaction (PCR) primer pair (forward: 5′-CGTCATGACCATGAACTTTCTGCTGT-3′; reverse: 5′-CCCAAGCTTCACCGCCTCGGCTTGTC-3′), respectively. PCR primer pair (forward: 5′-CATGCCATGGCAGCTATG AGGATCCAT-3′; reverse: 5′-CCGGAATTCTCAGGGTTTT TATTTCT-3′) was used for amplifying hBD3 cDNA from human gum tissues. The *Nco*I and *Eco*RI sites were introduced to the 5′ end and 3′ end of the hBD3 cDNA, respectively. $hVEGF_{165}$ and hBD3 cDNA were then cloned into the eukaryotic expression plasmid pVIVO1-mcs (InvivoGen, San Diego, CA) at the corresponding endonuclease sites to generate two recombinant plasmids. The plasmid pVIVO1-$hVEGF_{165}$-hBD3 contains the $hVEGF_{165}$ cNDA and the hBD3 cDNA, and the plasmid pVIVO1-$hVEGF_{165}$ only includes the $hVEGF_{165}$ cDNA. All the sequences were verified.

Flow cytometry analysis of BMSCs

Rat BMSCs were isolated and cultured in accordance with the standard methods (20).

BMSCs after three passages were trypsinised and harvested by centrifugation at 450 *g* for 5 minutes. The cells were resuspended and washed three times with phosphate-buffered saline (PBS) containing 1% bovine serum albumin (BSA). Monoclonal antibodies for CD34, CD44 and CD105 (Santa Cruz Biotechnology, Santa Cruz, CA) were incubated with the washed cells. Normal mouse IgG was used as an isotype control. After 45 minutes of incubation on ice in the dark, the cells were washed three times with 1% BSA/PBS, then resuspended in 0·5 ml 1% BSA/PBS and analysed by fluorescence-activated cell sorting (FACS).

Transfection of BMSCs

Purified BMSCs were inoculated into 75-cm^2 flasks at 2×10^6 cells/flask 1 day before transfection. Transfection was carried out when cells reached 60% confluence, and JetPEI transfection kit (Polyplus-transfection, NY) was used according to the manufacturer's instructions and Li's methods (21). BMSCs were divided into four groups for the transfections: N-BMSCs, untransfected control; T-BMSCs, cells transfected with pVIVO1-$hVEGF_{165}$-hBD3; C1-BMSCs, cells transfected with pVIVO1-$hVEGF_{165}$; and C2-BMSCs, cells transfected with pVIVO1-mcs (mock).

Western blot analysis

Twenty-four hours after transfection, the medium was changed to non-serum medium and the culture was continued for another 24 hours, then conditioned media (CM) of the above-mentioned four groups were collected and correspondingly named as N-CM, T-CM, C1-CM and C2-CM. Proteins were concentrated from the CM using protein concentration kit II (Applygen Technologies Inc., Beijing, China). Total protein level was quantified by bicinchoninic acid (BCA) protein quantification kit (Beyotime Institute of Biotechnology, Shanghai, China). The concentrated proteins (40 μg of proteins per lane) were subjected to sodium dodecyl sulfate-polyacrylamide gel exlectrophoresis (SDS-PAGE) and

transferred onto a nitrocellulose membrane, which was then incubated with a rabbit-anti-hVEGF antibody (1:500, Beyotime Institute of Biotechnology) and a goat-anti-hBD3 antibody (1:200, Santa Cruz Biotechnology), followed by incubation with the corresponding secondary antibodies. The bands were visualised by BeyoECL Plus (Beyotime Institute of Biotechnology).

Cell proliferation assay

Cell proliferation assay was performed with human endothelial cell EA.hy926 in RPMI-1640 medium containing 10% foetal bovine serum. EA.hy926 cells were inoculated into 96-well plates (4×10^3 cells/well, 100 μl/well). After 24 hours of conventional culture, the medium was replaced with one of the four above-mentioned CMs (six wells per group per day) and cell proliferation was monitored using CCK-8 kit (Dojindo, Kumamoto, Kyushu, Japan) for 5 days. In brief, each well was added with 10 μl of CCK-8 solution, followed by 3-hour incubation. The optical density was measured at 450 nm and day 0 was set as the baseline. To confirm whether the secreted $hVEGF_{165}$ can stimulate cell proliferation, an anti-$hVEGF_{165}$ neutralising antibody group (T-CM/Ab) was set. For this group, the $hVEGF_{165}$ neutralising antibody (final concentration 10 μg/ml; Abcam, Cambridge, UK) was added in the T-CM to inhibit $hVEGF_{165}$.

Wound-healing assay

EA.hy926 cells were inoculated into 12-well plates. On 95% confluence, a cross was scribed on the bottom of each well by a 1 ml sterile pipette to scratch the monolayer cells, followed by two washes with PBS to remove suspending cells. Each well was then added with 1 ml of the above-mentioned CM. An anti-$hVEGF_{165}$ neutralising antibody group was also set as mentioned earlier to determine the migration-promoting effect of $hVEGF_{165}$. At 0, 4, 8, 12 and 18 hours after scratching, a fixed field on each side of the cross was photographed under microscope (eight fields per time point per group). The healing ratio (HR) was determined by image analysis software TScratch-win (ETH Zurich, Zurich, Switzerland) (22). $HR = (A_0 - A_t)/A_0 \times 100\%$ (A_0, initial scratch area; A_t, residual wound surface at a specified time point). All analyses were carried out in a blind manner at least thrice by investigators not involved in this study.

Kleihauer–Betke method

Twentyfold CM concentrates were prepared by lyophilisation and resolvation. Round sterile filter paper pieces were immersed into the CM concentrates, and then placed onto Luria–Bertoni and Sabouraud agar plates containing *Escherichia coli*, *Pseudomonas aeruginosa*, *Staphylococcus aureus*, *Bacillus subtilis* and *Candida albicans*. After 10- to 12-hour incubation at 37/30°C, the plates were photographed. The size of the bacteriostasis ring around the filter paper piece was analysed to indicate the intensity of antibacterial activity.

Experimental animals and wound model

Three-month-old Sprague-Dawley (SD) rats, weighing 180–220 g, were obtained from the centre of experimental animal in our university (qualified certification number: CQA 0101015# and 0103017#, Chongqing, China). The experimental protocol used in this study was approved by the Animal Care Committee of our university and was in agreement with the 'Guide for the Care and Use of Laboratory Animals' published by the National Institutes of Health.

Rats were placed into a specially designed Plexiglass box and irradiated by ^{60}Co γ-ray (6 Gy/whole body). Within 30 minutes of irradiation, the rats were anesthetised by intraperitoneal injection with sodium pentobarbital (40 mg/kg), and the hair on the rats' back was shaved. A round full-thickness skin defect (18 mm in diameter) was made in the back of each rat using a homemade puncher (approximately 2% of whole body skin area) (23). The rats were then randomised into four groups (13 rats/group) as follows: group T, the rats received T-BMSCs; group C, the rats received C1-BMSCs; group N, the rats received N-BMSCs; and group S, the rats received PBS instead of BMSCs. Each rat was injected with 1 ml of BMSCs or PBS. A total of 1×10^7 cells were injected subcutaneously around the wound, and four injection sites were selected for each wound.

Assessing wound healing *in vivo*

To monitor the wound-healing process, the treated rats were raised separately. A digital camera was used to record the images of residual wound surface area on day 3, 7, 13 and 20 after preparation of the wound under the same photographic conditions. Meanwhile, the average healing time was calculated for each group. The data were analysed by investigators who were blind to the groups. A wound was considered healed when the scar was shed off and the wound was completely re-epithelialised, even if the surface was not completely covered with hair. The ratio of residual area to the original area was analysed using image analysis software. Pathologic study of the wound was carried out in 10 rats per group. One rat was euthanised on day 1 after preparation of the wound, and three rats were euthanised on days 7, 13 and 20 after preparation of the wound. The tissue specimens of the wound surface were collected and each specimen was separated into three fractions. The specimens were fixed in formalin, embedded in paraffin, sliced and stained with haematoxylin–eosin.

Immunohistochemical staining and Sirius red staining

For immunohistochemical staining, paraffin-embedded sections (4-μm thick) were dewaxed and rehydrated. For the detection of $hVEGF_{165}$ expression, the sections were then blocked with 5% BSA and incubated with an anti-hVEGF antibody (1:500) at 4°C for 12 hours, followed by incubating with an horseradish peroxidase (HRP)-conjugated goat-anti-rabbit IgG secondary antibody at 37°C for 30 minutes. For the detection of hBD3 expression, an anti-hBD3 antibody (1:200) was used as the primary antibody and an

HRP-conjugated rabbit-anti-goat IgG antibody was used as the secondary antibody. For the detection of laminin in wound area, the sections were blocked with normal goat serum after rehydration, incubated with an anti-laminin antibody (Zhongshan Goldenbridge, Beijing, China) at 4°C overnight, and then incubated with an HRP-conjugated goat-anti-rabbit IgG antibody for detecting. The 3,3′-diaminobenzidine (DAB) substrate was used for colorimetric detection.

Sirius red staining was performed as described (24). In brief, paraffin-embedded tissue sections were dehydrated and stained with Sirius red solution for 1 hour. Collagen fibril thickness and alignment were observed under polarising microscopy. The greyscale value of collagen fibril was determined using Image-Pro Plus software in a blind manner.

Statistical analysis

The data were processed by SPSS13.0. Group differences were analysed with the general linear model. Homoscedasticity was tested by Levene's test. Differences among multiple groups were analysed by Tukey's Honestly Significant Difference (HSD test and Dunnett's T3 test. All data are provided as mean ± SD. $P < 0{\cdot}05$ was considered statistically significant. All statistical graphs were plotted using GraphPad Prism software (GraphPad Software, San Diego, CA).

Results

Expression of hVEGF$_{165}$/hBD3 in BMSCs

BMSCs are positive for CD44 and CD105 and negative for CD34. We determined the purity of isolated rat BMSCs by flow cytometry; 96·36% of the cells were CD44+/CD34- and 94·57% of the cells were CD105+/CD34-, demonstrating high purity of the rat BMSCs. The recombinant plasmids pVIVO1-hVEGF$_{165}$-hBD3 and pVIVO1-hVEGF$_{165}$ were transfected into rat BMSCs, and the expression of hVEGF$_{165}$ and hBD3 in BMSCs was analysed by RT-PCR (Figure 1A). The band of hVEGF$_{165}$ was found in BMSCs transfected with mock (group C2) and the untransfected BMSCs (group N), but there was higher hVEGF$_{165}$ expression level in pVIVO1-hVEGF$_{165}$-hBD3 (group T) and pVIVO1-hVEGF$_{165}$ (group C1) transfected BMSCs, suggesting successful expression of the transfected hVEGF$_{165}$ gene in the cells. And, as expected, the expression of hBD3 was detected only in group T. The expression of the transfected genes was also confirmed by Western blot analysis of the CM from the four groups (Figure 1B). A band of 23-kDa hVEGF$_{165}$ protein was detected in all four groups, and a higher expression level of hVEGF$_{165}$ was found in groups T and C1. There was more than twice as much VEGF protein in T-CM as that in N-CM and C2-CM. The expression of the 5-kDa hBD3 protein was detected only in group T. The results were consistent with those of RT-PCR analysis, indicating that hVEGF$_{165}$ and hBD3 proteins were expressed successfully in the transfected BMSCs.

Functional characterisation of hVEGF$_{165}$/hBD3 proteins

To evaluate the efficacy of hVEGF$_{165}$ on cell proliferation, we performed a cell proliferation assay. According to the cell growth curves, T-CM and C1-CM significantly promoted cell proliferation from days 1 to 4 compared with C2-CM and N-CM ($P < 0{\cdot}05$; Figure 2A). To further confirm the efficacy of hVEGF$_{165}$ in T-CM, we added an anti-hVEGF$_{165}$ neutralising antibody in T-CM (T-CM/Ab) to block hVEGF$_{165}$ in the medium. As a result, cell proliferation was significantly suppressed after addition of the neutralising antibody ($P < 0{\cdot}05$). It demonstrates that hVEGF$_{165}$ in T-CM stimulated cell proliferation. No significant differences were found between T-CM and C1-CM and among T-CM/Ab, C2-CM and N-CM. We then carried out a monolayer cell-scratching assay to assess the efficacy of different CM on wound healing. At 4, 8, 12 and 18 hours after scratching, the HR of T-CM- and C1-CM-treated cells were significantly higher than that of C2-CM-, N-CM- and T-CM/Ab-treated cells ($P < 0{\cdot}05$, Figure 2B). At 18 hours after scratching, the cells in T-CM and C1-CM covered almost the whole wound surface, while only half of the wound surface was covered by the cells in C2-CM and N-CM. Cells in T-CM/Ab covered about 80% of the wound surface

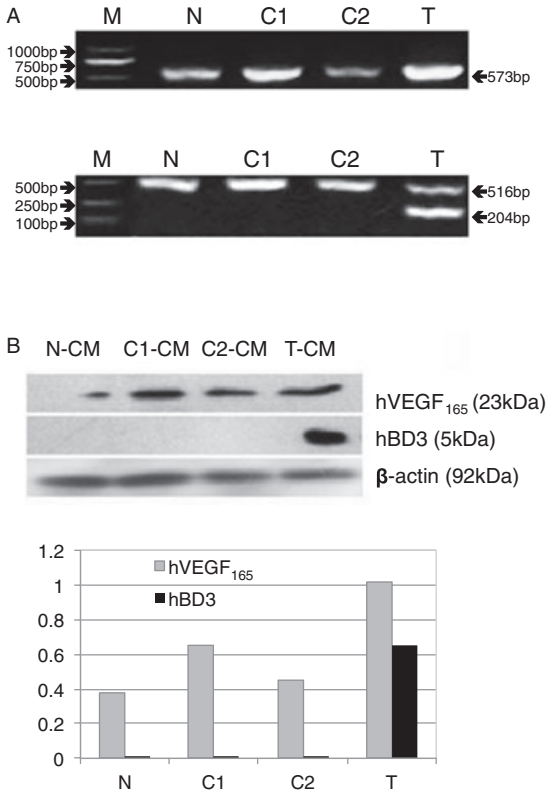

Figure 1 The expression of exogenous hVEGF$_{165}$/hBD3 in BMSCs. (A) RT-PCR analysis of transfected genes. Upper panel: PCR fragments of hVEGF$_{165}$; lower panel: PCR fragments of hBD3 (204 bp) and GAPDH (516 bp) as the internal control. N, N-BMSCs; C1, C1-BMSCs; C2, C2-BMSCs; T, T-BMSCs. (B) Western blot analysis of proteins secreted by BMSCs. Conditioned media (CM) collected from cultured BMSCs was blotted (N-CM, untransfected BMSCs; C1-CM, pVIVO1-hVEGF$_{165}$-transfected BMSCs; C2-CM, pVIVO1-mcs-mock-transfected BMSCs; T-CM, pVIVO1-hVEGF$_{165}$-hBD3-transfected BMSCs). The expected 23-kDa hVEGF$_{165}$ and 5-kDa hBD3 proteins were detected. β-Actin was used as a loading control. Densitometric quantification of proteins comparing with the β-actin was shown in the lower panel.

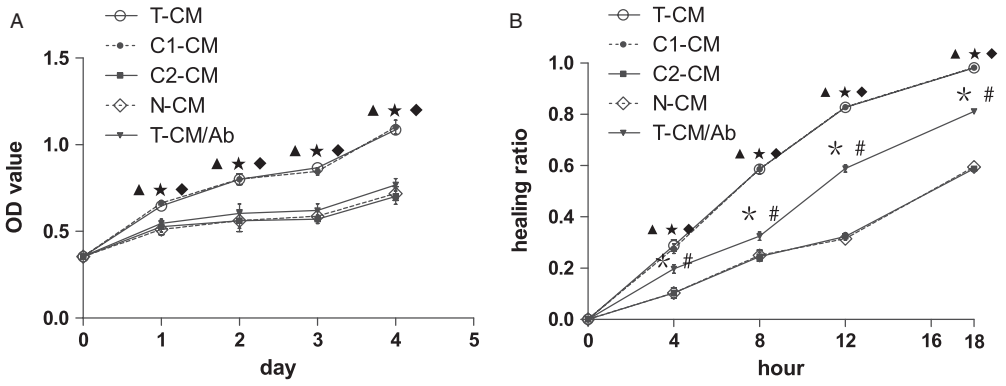

Figure 2 Function of BMSCs expressing exogenous $hVEGF_{165}$/hBD3. (A) Proliferation-promoting effect of different CMs. The cell growth curves revealed that T-CM and C1-CM significantly promoted cell proliferation from days 1 to 4, compared with C2-CM, N-CM and T-CM/Ab. The addition of anti-$hVEGF_{165}$ neutralising antibody to T-CM inhibited cell growth significantly. (B) *In vitro* wound-healing assay on monolayer of cells. The HR was significantly higher for cells treated with T-CM and C1-CM at 4, 8, 12 and 18 hours. The anti-$hVEGF_{165}$ neutralising antibody (T-CM/Ab) significantly inhibited T-CM-stimulated wound healing, but still did not abolish the effect of T-CM on wound healing. The HR was significantly higher for T-CM/Ab-treated cells than C2-CM- and N-CM-treated cells at 4, 8, 12 and 18 hours. No significant differences were found between T-CM and C1-CM and between C2-CM and N-CM. ▲$P < 0{\cdot}05$ T-CM or C1-CM versus C2-CM, ★$P < 0{\cdot}05$ T-CM or C1-CM versus N-CM, ◆$P < 0{\cdot}05$ T-CM or C1-CM versus T-CM/Ab, *$P < 0{\cdot}05$ T-CM/Ab versus C2-CM, #$P < 0{\cdot}05$ T-CM/Ab versus N-CM.

area, the HR was still significantly higher than that of C2-CM- and N-CM-treated cells ($P < 0{\cdot}05$). The results indicate that T-CM and C1-CM significantly accelerated wound healing, and the anti-$hVEGF_{165}$ neutralising antibody significantly inhibited this effect, but still did not abolish the efficacy of T-CM on wound healing. The overexpressed $hVEGF_{165}$ in the media has the activity of accelerating wound healing.

To test whether exogenously expressed hBD3 possesses antibacterial and antifungal activities, we performed a Kleihauer–Betke assay. Two gram-negative bacteria (*E. coli* and *P. aeruginosa*), two gram-positive bacteria (*S. aureus* and *B. subtilis*), and one common pathogenic fungus (*C. albicans*) were chosen for the test. There were clear bacteriostasis rings around the filter paper disks containing T-CM concentrates, indicating antibacterial and antifungal activity of T-CM. The other three concentrated CM did not show any antimicrobial activity (Figure 3). The results suggest the successful expression of hBD3 in T-BMSCs and that hBD3 protein secreted by T-BMSCs is biologically active.

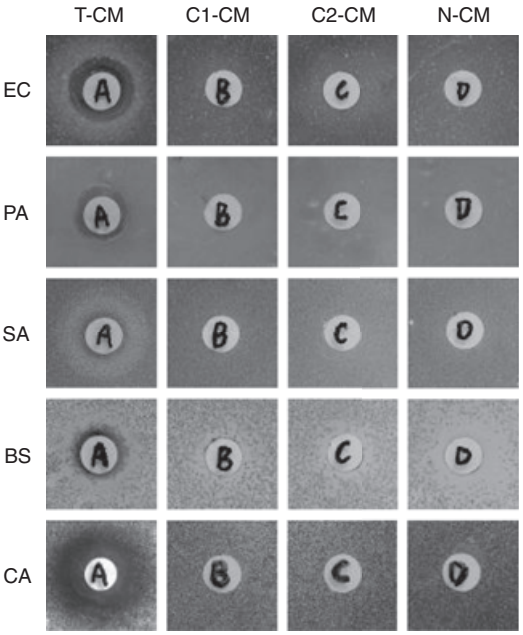

Figure 3 Antimicrobial effect of secreted hBD3 *in vitro*. Microorganisms on plates were treated with four concentrated CM in filter paper disks. The bacteriostasis ring around the filter paper disk was only found in T-CM-treated plates. EC, *Escherichia coli*; PA, *Pseudomonas aeruginosa*; SA, *Staphylococcus aureus*; BS, *Bacillus subtilis*; CA, *Candida albicans*.

Transplantation of $hVEGF_{165}$/hBD3-modified BMSCs accelerated wound healing

The rat model for combined radiation-wound injury was prepared by whole-body ionising irradiation (6Gy) plus excision of 2% full-thickness skin of the whole-body skin surface area. The simple skin excisional wound without radiation has a regular healing time of 17–18 days in rats (23). In our combined radiation-wound injury rat model, the average healing time was 24–25 days in the BMSC-treated group (group N) and 27–28 days in the PBS-treated group (group S), while in the T-BMSC-treated group (group T) and the C1-BMSC-treated group (group C), the average healing times were shortened to 20 days and 22–23 days, respectively. The wound was almost invisible in group T on day 20 after transplantation, while it was still clear in other three groups, especially in group S (Figure 4A). At days 7, 13 and 20 after cell transplantation, group S had the most residual wound surface area and the residual wound surface area in group N was significantly lower than that in group S ($P < 0{\cdot}05$; Figure 4B), suggesting that the transfection of untransfected BMSCs alone promoted wound healing. At days 13 and 20 after cell transplantation, the residual wound surface area in group C was significantly lower than that of groups N and S ($P < 0{\cdot}05$),

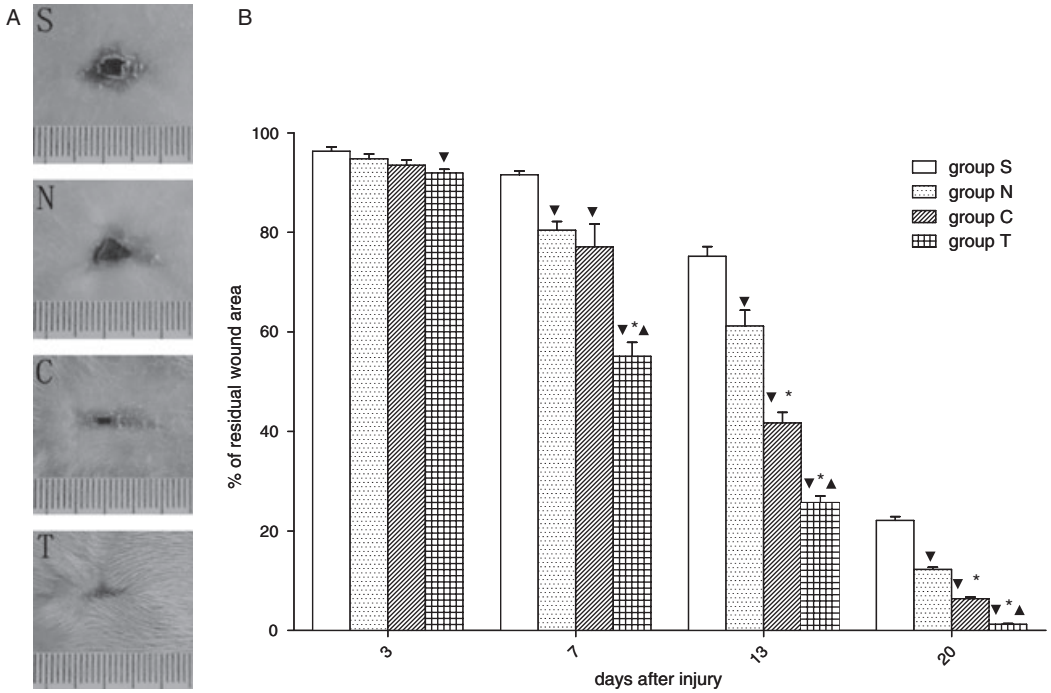

Figure 4 hVEGF$_{165}$/hBD3 promotes wound healing *in vivo*. (A) Representative pictures of wound healing on day 20 after BMSC injection. The wound was almost invisible in group T, whereas it was still visible in the other three groups, especially in group S (PBS control). (B) Comparison of residual wound area between different groups ($n = 6$). At day 7 and thereafter, group S had the most residual wound area and group T had the least residual wound area. The order of the four groups was S > N > C > S. ▼$p < 0{\cdot}05$ versus group S, *$P < 0{\cdot}05$ versus group N, ▲$P < 0{\cdot}05$ versus group C.

revealing that the overexpression of hVEGF$_{165}$ in BMSCs further accelerated wound healing. At days 7, 13 and 20 after cell transplantation, the residual wound surface area in group T was significantly lower than that of the other groups ($P < 0{\cdot}05$), demonstrating that exogenous hVEGF$_{165}$/hBD3 proteins accelerated wound healing from very early days. The fact that scar shedding and re-epithelialisation occurred earlier in group T than in group C indicates that hBD3 affected wound healing, possibly because of its antimicrobial activity.

Haematoxylin–eosin staining of wound tissues demonstrated well-organised granulation tissues in group T (Figure 5). The epithelial cells proliferated 7 days after injury, and multi-layer granulation tissues were observed in the centre of the wound surface. There were many microvessels in the granulation tissues of groups T and C, while no angiogenesis was observed in groups N and S at the same time. Blood congestion and haemorrhage were apparent in group S, mild in groups C and N, and rare in group T. On day 13 after injury and treatment, granulation tissues in group T were largely replaced by fibroblasts and newlyformed red-stained collagen fibres. Moreover, the wound surface was virtually covered by epithelia. The epithelial layer was significantly thicker in group T than in group N. As for group S, the formation of granulation tissues was still in progress. Twenty days after injury and treatment, the wound surface of group T was completely covered by new epithelial tissues with regenerated skin appendages, but less skin appendages were found in groups C and N and no skin appendages appeared in group S. The granulation tissue in group T was more matured than that in the other three groups.

Transplantation of hVEGF$_{165}$/hBD3-modified BMSCs facilitated angiogenesis, epithelialisation and collagen deposition and maturation in wound healing

One of the important functions of VEGF is the stimulation of angiogenesis during wound healing. Angiogenesis is a process that includes several key steps, including vasodilatation, basement membrane degradation, endothelial cell migration and proliferation, capillary formation and networking (vessel circuit formation) and new basement membrane formation (12,25). Laminin is a marker of the formation of vascular basement membrane. At the early stage of wound healing (the first 7 days after injury), the expression of laminin in the granulation tissue of the wound surface was significantly strong and widespread in groups T and C, but it was limited in groups N and S (Figure 6A, upper panels). On day 20 after injury, the laminin expression was still very strong and widespread in the granulation tissue of groups T and C, indicating the formation of large vessels. Laminin expression was strong within limited areas of the wound surface in groups N and S (Figure 6A, lower panels). The difference was significant between groups T and C and groups N and S (Figure 6B). The immunohistochemical staining of the day 7 sections indicates that the hVEGF$_{165}$ expression level in groups T and C was significantly higher than that in groups N and S (Figure 7A, upper panels, and B, left), and the hBD3 expression level in group T was significantly higher than that in the other three

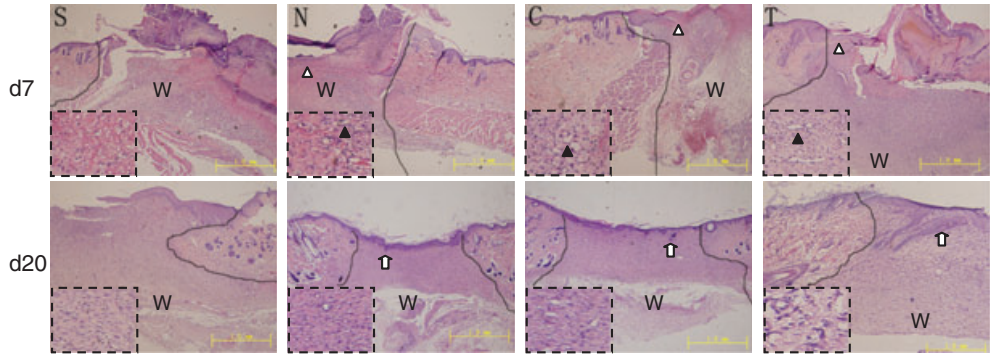

Figure 5 Histological studies on haematoxylin–eosin-stained radiation-wound tissues. The amplified local areas are shown in the dashed boxes. The comparable image of each group includes the wound edge and frontier of migrated epithelial cells. Upper panels: on day 7 after injury, blood congestion and haemorrhage were apparent in group S, mild in groups C and N and invisible in group T. Meanwhile, actively proliferating epithelial cells formed a multilayer structure (white triangle) and migrated to the centre of the nude wound. Angiogenesis in granulation tissues (black triangles) was clear in group T, mild in groups C and N and invisible in group S. Lower panels: on day 20 after injury and treatment, the wound was re-epithelialised completely with regenerated skin appendages (white arrows) in group T, but the re-epithelialisation and regeneration of skin appendages were less in groups C and N and invisible in group S. The lines indicate the interface of the wound and unaffected skin. W, wound site. Bars = 1 mm.

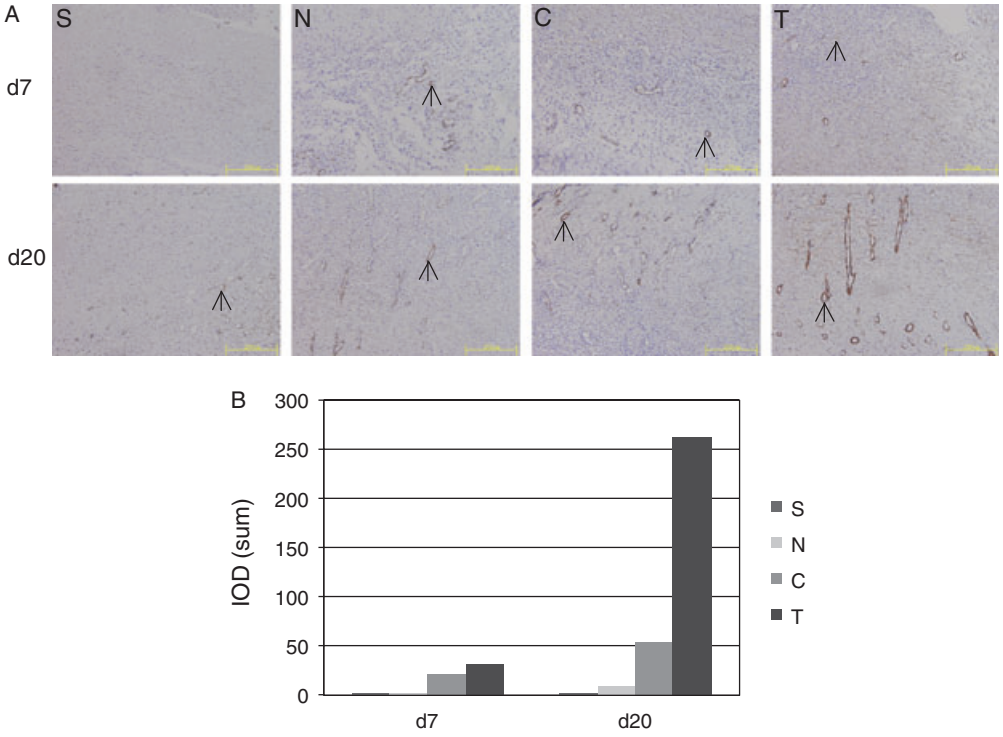

Figure 6 Laminin expression in vascular basement membrane of granulation tissue of wound surface. (A) Upper panels: on day 7 after injury, laminin expression (black arrows) was strong and widespread in granulation tissue of groups T and C. Laminin expression was positive but within limited areas in groups N and S. Lower panels: on day 20 after injury, laminin expression was still strong and widespread in groups T and C, suggesting the formation of large vessels. Laminin expression was strong but in limited areas in groups N and S. Bars = 200 μm. (B) Images were analysed for quantifying the laminin expression in granulation tissue.

groups (Figure 7A, lower panels, and B, right), indicating that $hVEGF_{165}$/hBD3-modified BMSCs expressed $hVEGF_{165}$ and hBD3 proteins successfully in the wound surface.

Sirius red staining was used to reveal the quantity and quality of collagen fibres, thus helping to elucidate the role of $hVEGF_{165}$/hBD3 in collagen formation during wound healing. Following Sirius red staining, the wound surface can be distinguished from the normal skin, which was bright red because of the large amount of collagens (Figure 8A). The results show that collagen fibres, mostly type I collagen, began to deposit from day 7 after injury. On day 20 after injury, there was more type I collagen in group T than in the other three groups, and the collagen layer was also thicker in group T. Besides, the collagen array and red refractive power were

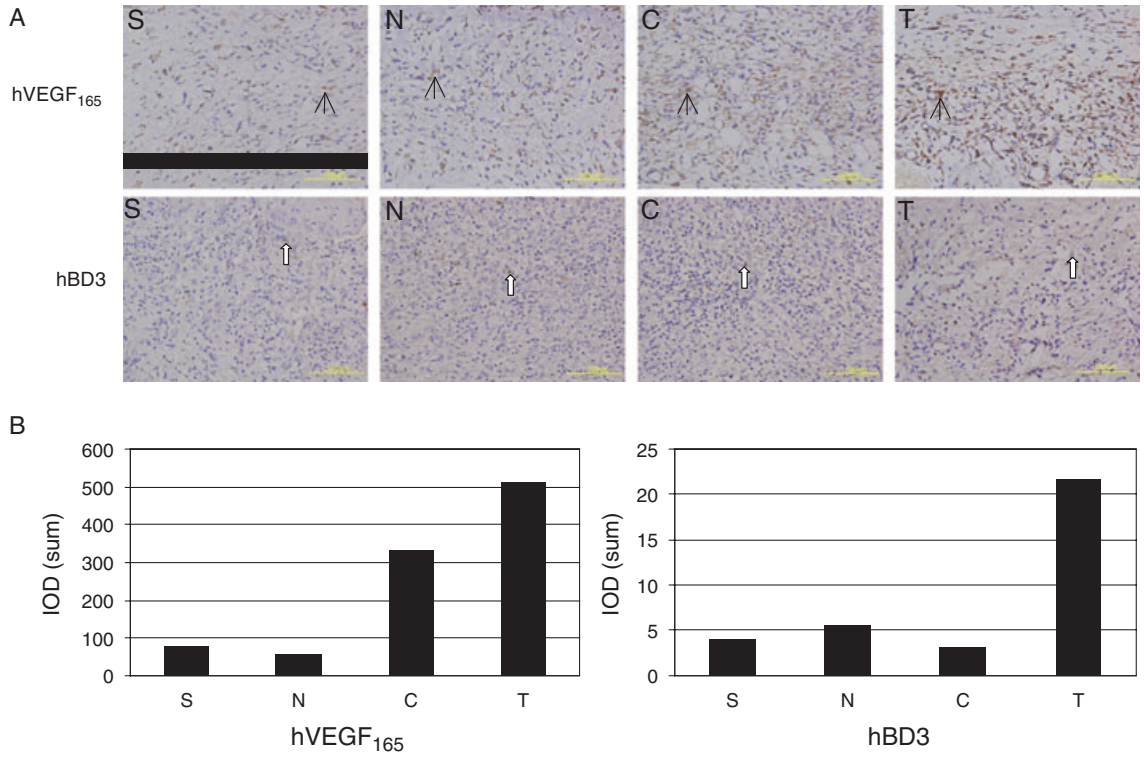

Figure 7 Immunohistochemical studies revealed $hVEGF_{165}$/hBD3 expression in the granulation tissue on day 7 after injury. (A) Upper panels: the $hVEGF_{165}$ expression (black arrows) was strong in groups T and C. Lower panels: the hBD3 expression (white arrows) was strong in group T. Bars = 100 μm. (B) Images were analysed for quantifying $hVEGF_{165}$/hBD3 expression in granulation tissue.

similar to the normal skin in group T but not in the other three groups. From days 7 to 20, the collagen content of group T was significantly higher than that of the other groups ($P < 0{\cdot}05$) and there were significant differences between groups ($P < 0{\cdot}05$), the order was group T > group C > group N > group S (Figure 8B).

Discussion

Impaired healing process and prolonged healing time is a tough problem of combined radiation-wound in clinical practice and a significant burden to patients. Recently, stem cell therapy was proposed as an addition to conventional surgical therapy in the treatment of chronic radiation injuries (26). A patient with severe radiation burns was successfully treatment by local autologous BMSC administration (27). Akita *et al*. (28) treated a radiation-injured patient using non-cultured autologous-adipose-derived stem cells together with basic fibroblast growth factor. These studies suggest possible clinical application of stem cells in radiation-wound injuries. BMSC was also demonstrated in favour of radiation-wound healing in a minipig model (29). Growth factors and cytokines can promote chronic wound healing by stimulating cell proliferation and angiogenesis in the wounds. Therefore an *ex vivo* gene therapy strategy of overexpressing growth factors and cytokines in BMSCs was proposed. It is reasonable to expect that genes encoding growth factors and cytokines exhibit great reparative potential to accelerate wound closure (30). In Hao's studies, BMSCs overexpressing hPDGF-A and hBD2 accelerated wound healing of combined radiation-wound injury (23). Yan *et al*. (31) in our institute have demonstrated that human-platelet-derived growth factor A-modified BMSCs promoted the healing of combined radiation-wound injury in minipigs. To search for more genes with better efficacies, we used a strategy that combines wound-healing promotion and immunological improvement. $hVEGF_{165}$ is an angiogenesis stimulator and hBD3 acts as an immune enhancer. The former can specifically induce endothelial cell proliferation and angiogenesis, so as to promote wound healing, the latter has antibacterial and antifungal activities and can be used to neutralise toxins. The combination of these two factors could be of benefit to wound healing. In this study, we successfully coexpressed $hVEGF_{165}$ and hBD3 in BMSCs and demonstrated that this combination accelerated the healing of combined radiation-wound injury and improved the quality of healing.

We used a eukaryotic expression plasmid as the vector to express $hVEGF_{165}$ and hBD3 in BMSCs for the following reasons: (i) This virus-free vector does not integrate into host chromosomes, so there is no risk of insertion mutation and oncogenicity. (ii) The plasmid contains two transcription units and two promoters, allowing the high-level coexpression of two genes *in vivo*. (iii) The gene expression is transient after transfection and would be expected to cease after closure of the wound surface, so the risks caused by overlong expression of the transfected genes could be limited. This is especially

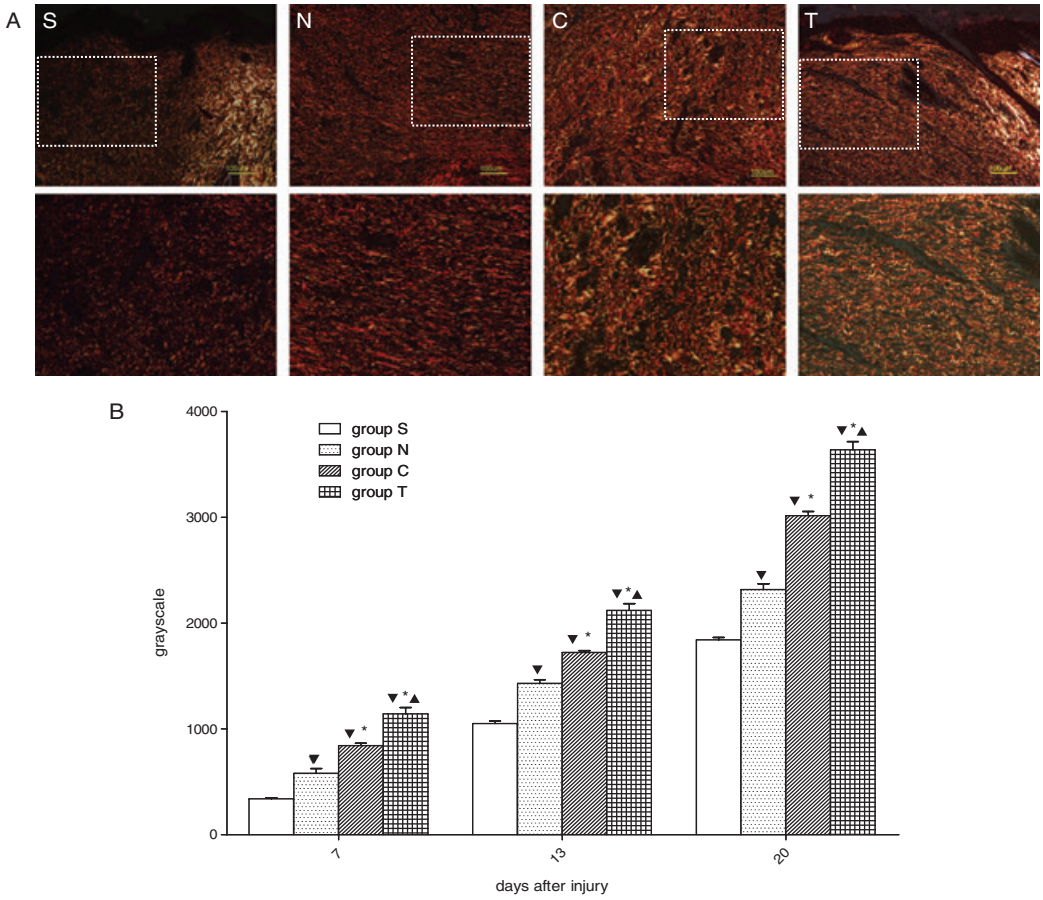

Figure 8 Collagen deposition in wound sites after injury. (A) Representative collagen staining of sections from different groups. Type I collagen is shown in yellow, orange and red, type II collagen is shown in various colours and type III collagen is shown in green. The normal dermis (bright area) was easily distinguished from the wound skin (dark area). The dashed squares in the upper panels are amplified in the corresponding lower panels. Compared with the other three groups, there were much more type I collagen fibres in group T, and the fibres were also thicker. Bars = 100 μm. (B) Collagen contents in wound tissue. The total collagen content was indicated by average greyscale value. From days 7 to 20, the average greyscale value of group T was significantly higher than that of the other groups. Likewise, group C was significantly higher than groups N and S, and group N was significantly higher than group S. ▼$P < 0{\cdot}05$ versus group S, *$P < 0{\cdot}05$ versus group N, ▲$P < 0{\cdot}05$ versus group C.

essential if the transfected genes code for growth factors. (iv) Virus-free vectors are less immunogenic than viral vectors.

New strategies to promote wound healing are aimed at replacing senescent inherent cells and restore normal cell cycle (32,33). BMSCs have become an attractive candidate in cell therapy because they can differentiate into various cell types, suppress activation and proliferation of immune cells and contribute to tissue repair and reconstruction via various paracrine mechanisms (7,34). VEGF induces mesenchymal stem cells to differentiate into endothelial-cell-like cells, which express kinase insert domain-containing receptor (KDR), fms-related tyrosinekinase 1 (FLT-1) and von Willebrand factor and form capillary-like structures. *In vitro* studies have demonstrated that BMSCs can secrete VEGF, basic fibroblast growth factor (bFGF),, angiogenin, procathepsin B, interleukin-11 (IL-11) and bone morphogenetic protein (BMP); these factors can influence the migration, extracellular matrix invasion, proliferation and survival of endothelial cells (35–37). The efficacy of BMSCs alone in promoting wound healing was demonstrated in our studies. In the rat combined-radiation injury model, the untransfected BMSCs significantly accelerated wound healing compared with the PBS control. This is in agreement with previous studies. Nevertheless, we also demonstrated that the gene-modified BMSCs promoted wound healing more efficiently than did the untransfected BMSCs. The average healing time was shortened from 27 to 28 days in untreated rats (group S) to 20 days in treated rats (group T), which was very close to the normal healing time. Comparing the quality of granulation tissue formation and collagen deposition, the groups present the following order: $hVEGF_{165}$/hBD3-modified BMSCs > $hVEGF_{165}$-modified BMSCs > untransfected BMSCs > PBS control. This is in accordance with the order of average healing time of the four groups. The same order was also demonstrated by histological studies. Among the four groups, group T exhibited the least haemorrhage and congestion, the most cellular components and newly formed vessels in granulation tissue at the early stage of wound healing, and the most appendages of the skin and mature collagen deposition at the late stage of wound healing. These results demonstrate that the

ex vivo expression of $hVEGF_{165}$ and hBD3 improved wound healing.

Bacterial infection in the open wound is a severe problem at the early stage of wound healing. An antimicrobial agent could help resist infections and is beneficial for wound healing. hBD3 was demonstrated to possess antimicrobial effect in our *in vitro* experiments. In the *in vivo* studies, $hVEGF_{165}$/hBD3-modified BMSCs exhibited better efficacy than did $hVEGF_{165}$-modified BMSCs in all the tested items, suggesting that the double-gene-modified BMSCs accelerated wound healing more efficiently than did the single-gene-modified BMSCs. These results provide the evidence that hBD3 plays certain roles in wound healing; it possibly relates to its antimicrobial activity. The studies demonstrate that combination of $hVEGF_{165}$ and hBD3 has a synergistic effect on promoting wound healing in such a way that the two proteins act via different mechanisms.

In summary, we used a eukaryotic expression plasmid to express $hVEGF_{165}$ and hBD3 genes in BMSCs, which were then transplanted into the site of the combined radiation-wound injury. The results demonstrated that coexpression of $hVEGF_{165}$ and hBD3 in BMSCs significantly accelerated wound healing. Our studies suggest that this gene therapy strategy is a promising approach in the treatment of refractory wounds.

Acknowledgements

This study was supported by the National Natural Science Foundation of China (no.30670636) and the Natural Science Foundation of Chongqing Municipality of China (no.2006 BB5095).

References

1. Kang MH, Kim DY, Yi JY, Son Y. Substance Paccelerates intestinal tissue regeneration after gamma-irradiation-induced damage. *Wound Repair Regen* 2009;**17**:216–23.
2. Yu J, Piao BK, Pei YX, Qi X, Hua BJ. Protective effects of tetrahydropalmatine against gamma-radiation induced damage to human endothelial cells. *Life Sci* 2010;**87**:55–63.
3. Hu SY, Duan HF, Li QF, Yang YF, Chen JL, Wang LS, Wang H. Hepatocyte growth factor protects endothelial cells against gamma ray irradiation-induced damage. *Acta Pharmacol Sin* 2009;**30**: 1415–20.
4. Goldman R. Growth factors and chronic wound healing: past, present, and future. *Adv Skin Wound Care* 2004;**17**:24–35.
5. Caplan AI. Adult mesenchymal stem cells for tissue engineering versus regenerative medicine. *J Cell Physiol* 2007;**213**:341–7.
6. Uccelli A, Pistoia V, Moretta L. Mesenchymal stem cells: a new strategy for immunosuppression? *Trends Immunol* 2007;**28**:219–26.
7. Hanson SE, Bentz ML, Hematti P. Mesenchymal stem cell therapy for nonhealing cutaneous wounds. *Plast Reconstr Surg* 2010;**125**: 510–6.
8. Dazzi F, Horwood NJ. Potential of mesenchymal stem cell therapy. *Curr Opin Oncol* 2007;**19**:650–5.
9. Gavard J, Gutkind JS. VEGF controls endothelial-cell permeability by promoting the beta-arrestin-dependent endocytosis of VE-cadherin. *Nat Cell Biol* 2006;**8**:1223–34.
10. Yoshida A, Nand-Apte B, Zetter BR. Differential endothelial migration and proliferation to basic fibroblast growth factor and vascular endothelial growth factor. *Growth Factors* 1996;**13**:57–64.
11. Leung DW, Cachianes G, Kuang WJ, Goeddel DV, Ferrara N. Vascular endothelial growth factor is a secreted angiogenic mitogen. *Science* 1989;**246**:1306–9.
12. Bao P, Kodra A, Tomic-Canic M, Golinko MS, Ehrlich HP, Brem H. The role of vascular endothelial growth factor in wound healing. *J Surg Res* 2009;**153**:347–358.
13. Brkovic A, Sirois MG. Vascular permeability induced by VEGF family members in vivo: role of endogenous PAF and NO synthesis. *J Cell Biochem* 2007;**100**:727–37.
14. Robson MC. Wound infection. A failure of wound healing caused by an imbalance of bacteria. *Surg Clin North Am* 1997;**77**:637–50.
15. Luenser K, Ludwig A. Variability and evolution of bovine beta-defensin genes. *Genes Immun* 2005;**6**:115–22.
16. Harder J, Meyer-Hoffert U, Wehkamp K, Schwichtenberg L, Schroder JM. Differential gene induction of human beta-defensins (hBD-1, -2, -3, and -4) in keratinocytes is inhibited by retinoic acid. *J Invest Dermatol* 2004;**123**:522–9.
17. Wu Z, Hoover DM, Yang D, Boulègue C, Santamaria F, Oppenheim JJ, Lubkowski J, Lu W. Engineering disulfide bridges to dissect antimicrobial and chemotactic activities of human beta-defensin 3. *Proc Natl Acad Sci U S A* 2003;**100**:8880–5.
18. Dhople V, Krukemeyer A, Ramamoorthy A. The human beta-defensin-3, an antibacterial peptide with multiple biological functions. *Biochim Biophys Acta* 2006;**1758**:1499–512.
19. Harder J, Bartels J, Christophers E, Schroder JM. Isolation and characterization of human beta -defensin-3, a novel human inducible peptide antibiotic. *J Biol Chem* 2001;**276**:5707–13.
20. Javazon EH, Colter DC, Schwarz EJ, Prockop DJ. Rat marrow stromal cells are more sensitive to plating density and expand more rapidly from single-cell-derived colonies than human marrow stromal cells. *Stem Cells* 2001;**19**:219–225.
21. Li W, Ma N, Ong LL, Nesselmann C, Klopsch C, Ladilov Y, Furlani D, Piechaczek C, Moebius JM, Lützow K, Lendlein A, Stamm C, Li RK, Steinhoff G. Bcl-2 engineered MSCs inhibited apoptosis and improved heart function. *Stem Cells* 2007;**25**:2118–27.
22. Geback T, Schulz MM, Koumoutsakos P, Detmar M. TScratch: a novel and simple software tool for automated analysis of monolayer wound healing assays. *Biotechniques* 2009;**46**:265–74.
23. Hao L, Wang J, Zou Z, Yan G, Dong S, Deng J, Ran X, Feng Y, Luo C, Wang Y, Cheng T. Transplantation of BMSCs expressing hPDGF-A/hBD2 promotes wound healing in rats with combined radiation-wound injury. *Gene Ther* 2009;**16**:34–42.
24. Junqueira LC, Cossermelli W, Brentani R. Differential staining of collagens type I, II and III by Sirius Red and polarization microscopy. *Arch Histol Jpn* 1978;**41**:267–74.
25. Gallin JI, Goldstein IM. Angiogenesis and inflammation. In: Gallin JI, Goldstein IM, Snyderman R, editors. *Inflammation: basic principles and clinical correlates*, 2nd edn. New York: Raven Press, 1992:821–39.
26. Lataillade JJ, Doucet C, Bey E, Carsin H, Huet C, Clairand I, Bottollier-Depois JF, Chapel A, Ernou I, Gourven M, Boutin L, Hayden A, Carcamo C, Buglova E, Joussemet M, de Revel T, Gourmelon P. New approach to radiation burn treatment by dosimetry-guided surgery combined with autologous mesenchymal stem cell therapy. *Regen Med* 2007;**2**:785–94.
27. Bey E, Prat M, Duhamel P, Benderitter M, Brachet M, Trompier F, Battaglini P, Ernou I, Boutin L, Gourven M, Tissedre F, Créa S, Mansour CA, de Revel T, Carsin H, Gourmelon P, Lataillade JJ. Emerging therapy for improving wound repair of severe radiation burns using local bone marrow-derived stem cell administrations. *Wound Repair Regen* 2010;**18**:50–8.
28. Akita S, Akino K, Hirano A, Ohtsuru A, Yamashita S. Noncultured autologous adipose-derived stem cells therapy for chronic radiation injury. *Stem Cells Int* 2010;**2010**:532704.
29. Agay D, Scherthan H, Forcheron F, Grenier N, Hérodin F, Meineke V, Drouet M. Multipotent mesenchymal stem cell grafting to treat cutaneous radiation syndrome: development of a new minipig model. *Exp Hematol* 2010;**38**:945–56.

30. Branski LK, Gauglitz GG, Herndon DN, Jeschke MG. A review of gene and stem cell therapy in cutaneous wound healing. *Burns* 2009;**35**:171–80.
31. Yan G, Sun H, Wang F, Wang J, Wang F, Zou Z, Cheng T, Ai G, Su Y. Topical application of hPDGF-A-modified porcine BMSC and keratinocytes loaded on acellular HAM promotes the healing of combined radiation-wound skin injury in minipigs. *Int J Radiat Biol* 2011;**87**:591–600.
32. Panuncialman J, Falanga V. The science of wound bed preparation. *Surg Clin North Am* 2009;**89**:611–26.
33. Herdrich BJ, Lind RC, Liechty KW. Multipotent adult progenitor cells: their role in wound healing and the treatment of dermal wounds. *Cytotherapy* 2008;**10**:543–50.
34. Hematti P. Role of mesenchymal stromal cells in solid organ transplantation. *Transplant Rev (Orlando)* 2008;**22**:262–73.
35. Oswald J, Boxberger S, Jørgensen B, Feldmann S, Ehninger G, Bornhäuser M, Werner C. Mesenchymal stem cells can be differentiated into endothelial cells in vitro. *Stem Cells* 2004;**22**:377–84.
36. Wu Y, Chen L, Scott PG, Tredget EE. Mesenchymal stem cells enhance wound healing through differentiation and angiogenesis. *Stem Cells* 2007;**25**:2648–59.
37. Potapova IA, Gaudette GR, Brink PR, Robinson RB, Rosen MR, Cohen IS, Doronin SV. Mesenchymal stem cells support migration, extracellular matrix invasion, proliferation, and survival of endothelial cells in vitro. *Stem Cells* 2007;**25**:1761–8.